Diffusion and clustering of Au adatoms on H-terminated Si(111)-(1×1): A first principles study

Soo-Hwan Lee and Gyeong S. Hwang[a)]
Department of Chemical Engineering, University of Texas, Austin, Texas 78713, USA

(Received 12 June 2009; accepted 21 September 2009; published online 13 October 2009)

We have examined the diffusion and agglomeration of Au adatoms on the H-terminated Si(111)-(1×1) surface using periodic slab density functional theory calculations. We find that a single Au atom favorably resides atop a surface Si atom by breaking an original ≡Si–H bond while the H atom is bonded to the Au atom in the vertical direction, leading to the ≡Si–Au–H state. Starting from the most favorable on-top (*T*) site, a Au adatom is predicted to undergo diffusion by moving in and out of the *T* site without disrupting surface Si–H bonds. The predicted overall activation energy for the Au diffusion is 0.5 eV. Our calculations show that Au agglomeration leads to libration of H atoms from the Au/Si interface, while the H atoms are weakly bound to Au clusters and subsequently undergo associative H_2 desorption with no significant barrier. Based on charge density analysis we also discuss bonding mechanisms for Au on H-terminated Si(111)-(1×1). Our findings are as a whole consistent with experimental results available in literature. © *2009 American Institute of Physics*. [doi:10.1063/1.3246167]

I. INTRODUCTION

The diffusion and agglomeration of metal adatoms on the H-terminated Si(111)-(1×1) and clean Si(111)-(7×7) surfaces have long been a subject of intensive investigation because of their technological and scientific importance. Precise control of the growth and structure of metal nanoparticles and thin films is essential to develop future nanodevices utilizing their unique properties. It is well known that the behavior of metal adatoms on Si is significantly influenced by the presence of surfactants, such as H atoms which can effectively terminate the dangling bonds of surface Si atoms. Surfactant-modified Si surfaces, compared to their clean counterparts, often result in a noticeable modulation in the morphology and growth mode of metal films[1–6] due largely to changes in the mobility of metal adatoms and the relative energetics between metal-substrate interfaces and metal overlayers. Therefore, a detailed understanding of how surfactant introduction affects metal adatom diffusion and metal-substrate interfacial interactions is necessary for well-controlled synthesis of Si-supported metal nanostructures.

In recent years, extensive studies have been undertaken to understand the fundamental phenomena occurring in the Au/Si system, such as Au growth on Si,[7] Si outdiffusion through a thin Au overlayer,[8] Au–Si alloy formation,[9] and Au-catalyzed Si nanowire growth.[10] Among some fundamental issues that still remain unclarified, one interesting feature is the effect of H-passivation on the diffusion of Au adatoms on Si and the stability of H atoms at the Au/Si interface. An earlier experimental study based on nuclear reaction analysis[11] showed that the mobility of Au adatoms is restricted, while H atoms appear to remain intact on the H-terminated Si(111)-(1×1) surface [Si(111)–H]. In addition, the study demonstrated liberation of H atoms from the Au/Si interface during Au deposition on Si(111)–H even at 110 K, as also proposed by other experimental studies based on high-resolution synchrotron photoemission[12] and scanning tunneling microscopy.[13] This is in direct contradiction to the behavior seen in the case of other metals such as Pb, Ag, and Cu in which H atoms preferentially remain at the metal/Si interface.[14] Moreover, the Si(111)–H surface is likely to produce significant mobility enhancement for various metal adatoms. For instance, recent first principles total-energy calculations[15] predicted a small diffusion barrier of 0.14 eV for Ag on Si(111)–H, as opposed to 0.88 eV on clean Si(111)-(7×7). The different behavior of Au is possibly related to the reactive nature of the Au/Si interface, yet the underlying atomistic mechanisms remain unclear.

In this paper, we present viable mechanisms for Au diffusion and agglomeration based on spin-polarized density functional theory (DFT) calculations on the H-terminated Si(111)-7×7 surface, and also discuss the stability of H atoms at the Au/Si interface. The fundamental findings could also assist in better understanding the behavior of Au atoms during the Au-catalyzed vapor-liquid-solid (VLS) growth of Si nanowires. A series of recent experiments[16–19] have evidenced the gradual shrinkage of Au droplets that remain at the tips of growing Si nanowires, and also the precipitation of Au particles on the Si nanowire sidewalls during cooling, which may in turn cause the termination of nanowire growth. Given the low equilibrium solubility of Au in bulk Si at typical VLS growth temperatures,[20] the loss of Au atoms from the droplets is expected to occur via migration along the nanowire sidewalls which often consist of H-passivated (111) facets.[10] Therefore, a better understanding of Au diffusion and agglomeration on H/Si(111) could further provide some insights into preventing such Au catalyst loss.

[a)]Author to whom correspondence should be addressed. Electronic mail: gshwang@che.utexas.edu. Tel.: 512-471-4847. FAX: 512-471-7060.

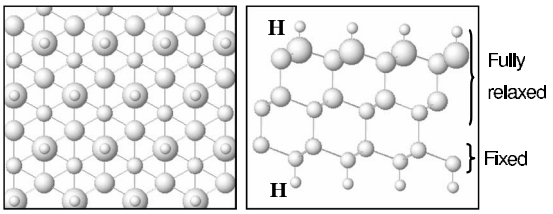

FIG. 1. Top (left panel) and side (right panel) views of the H-terminated Si(111)-(1×1) surface model employed in this work. The surface Si atoms are represented as the largest gray balls and the sublayer Si atoms are indicated by smaller balls for the sake of clarity. The smallest gray balls represent H atoms.

II. COMPUTATIONAL METHODS

All optimized atomic structures and energies reported herein were computed using a plane-wave basis set pseudopotential method within the generalized gradient approximation of Perdew and Wang[21] to spin-polarized DFT, as implemented in the well-established Vienna *ab initio* simulation package (VASP).[22–24] Vanderbilt-type ultrasoft pseudopotentials[25,26] were used for core-electron interactions. The valence configurations used to generate the ionic pseudopotentials are $5d^{10}6s^1$ for Au and $3s^23p^2$ for Si. Outer electron wave functions were expanded using a plane-wave basis set with a kinetic energy cutoff of 270 eV. The H-terminated Si(111)-(1×1) surface is modeled using a two-dimensional periodic slab with six atomic layers each of which contains 16 Si atoms, while the slab is separated from its vertical periodic images by a vacuum space approximately of 13 Å, as illustrated in Fig. 1. The bottom two layers are fixed in their bulk positions and the Si dangling bonds are passivated by H atoms. The remaining Si layers, surface H atoms, and Au adatoms are fully relaxed using the conjugate gradient method until residual forces on the movable atoms become smaller than 5×10^{-2} eV/Å. The Brillouin zone sampling was performed with a (2×2×1) Monkhost–Pack mesh of *k* points. Checking the convergence of our calculation results with respect to the *k*-point mesh size, plane-wave cutoff energy, and vacuum space, the chosen values turn out to be sufficient for describing Au diffusion and agglomeration on Si(111)–H. The nudged elastic band method[27] was used to determine the pathways and barriers of Au diffusion with eight intermediate images for each diffusion event considered.

III. RESULTS AND DISCUSSION

A. Adsorption

Figure 2 shows four sites that we considered for the adsorption of a neutral Au atom on the H-terminated Si(111) surface, including (a) onefold on-top site (indicated by *T* hereafter) in which Au resides atop a surface Si atom while breaking an original H–Si bond such that the dissociated H atom is attached to the Au atom, (b) twofold bridge site (*B*) in which Au is located above the middle of two Si surface atoms, (c) threefold filled site (*F*) in which Au is placed above the center of three Si surface atoms while having a first sublayer Si atom underneath, and (d) threefold hollow site (*H*) which is above a third sublayer Si atom. The *T* and *B* sites are identified to be stable adsorption sites, but the *F* and *H* sites turn out to be saddle points as discussed later. As summarized in Table I, the *T* site turns out to be most favorable with a Au adsorption energy of 0.91 eV, followed by the *B*, *F*, and *H* sites which are 0.26, 0.40, and 0.46 eV less favorable, respectively. Here, the Au adsorption energy (E_{ad}) is computed by

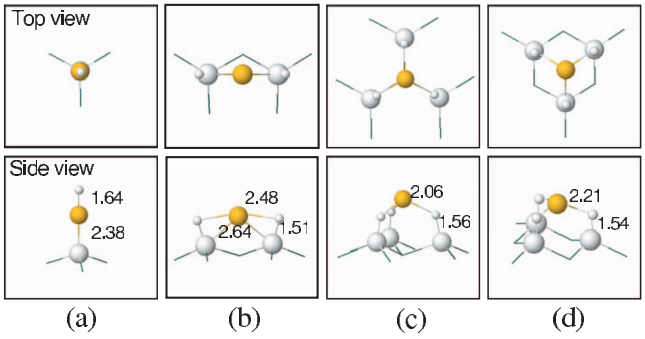

FIG. 2. Schematic representation of the minimum-energy adsorption configurations of Au on the H-terminated Si(111)-(1×1) surface: (a) Onefold on-top (indicated by *T* in the text), (b) twofold bridge (*B*), (c) threefold filled (*F*), and (d) threefold hollow (*H*). For each adsorption state, both top (upper panel) and side (lower panel) views are presented. The dark (yellow) gray, gray, and small white balls represent Au, Si, and H atoms, respectively. The bond lengths indicated are given in angstroms.

$$E_{ad} = E_{Au/Si(111)-H} - E_{Si(111)-H} - E_{Au},$$

where $E_{Au/Si(111)-H}$, $E_{Si(111)-H}$, and E_{Au} refer to the total energies of the Au/Si(111)–H adsorption system, the H-terminated Si(111) surface, and the gas-phase Au atom in the doublet state, respectively.

In addition, our calculation predicts the energy cost of neutral Au–H liberation from the *T* site to be around 1.4 eV, i.e., $\equiv$Si–Au–H$\rightarrow\equiv$Si·+Au–H(g), where dash (–) and dot (·) indicate a Si–Si bond and an unpaired electron, respectively. The sizable adsorption energies suggest that a neutral Au atom will stably exist on the Si(111)–H surface at moderate temperatures. We also calculated energy variations by placing a Au atom at several subsurface sites, but the result shows that the subsurface sites are roughly >1.2 eV

TABLE I. Calculated Au adsorption energies (in eV) at various sites. Here, the adsorption energy (E_{ad}) is given by $E_{ad}=E_{Au/Si(111)-H}-E_{Si(111)-H}-E_{Au}$, where $E_{Au/Si(111)-H}$, $E_{Si(111)-H}$, and E_{Au} refer to the total energies of the Au/Si(111)–H adsorption system, the H-terminated Si(111) surface, and the gas-phase Au atom in the doublet state, respectively. The *F* and *H* sites are identified to be saddle points, while the *T* and *B* sites are local minima (see text).

	Onefold on-top (*T*)	Twofold bridge (*B*)	Threefold filled (*F*)	Threefold hollow (*H*)
E_{ad}	0.91	0.65	0.51	0.45

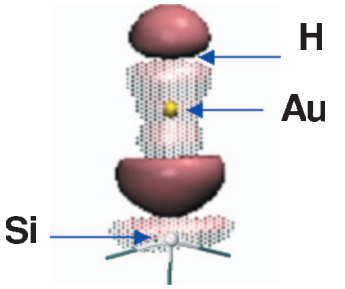

FIG. 3. Charge density difference plot for Au adsorption at the onefold on-top site. The charge density difference ($\Delta\rho$) is calculated by subtracting the charge densities of isolated Au and H atoms from the total charge density of the H–Au–Si≡ unit with no atomic displacement, i.e., $\Delta\rho = \rho_{H-Au-Si} - \rho_{Au} - \rho_{H}$. The positions of the surface Si, Au, and H atoms are indicated. The dark gray (brown) and gray isosurfaces represent the regions of charge gain and loss, respectively.

less favorable than the most favorable T site. This implies that single Au atoms would prefer to remain on the H/Si(111) surface, rather than diffusing into the Si substrate.

For Au adsorption at the T site, bonding mechanisms were analyzed based on charge density differences. As presented in Fig. 3, the result demonstrates some electron depletion around the surface Si atom and electron accumulation in the H atom, while the Au atom appears polarized with negative and positive charges toward the Si and H atoms, respectively. This may indicate existence of ionic-type Si–Au and Au–H interactions. In addition, as summarized in Fig. 4, our local density of states (LDOS) analysis shows unpaired spin populations with partial filling in the H lowest unoccupied molecular orbital and the Si highest occupied molecular orbital, implying the occurrence of partial electron transfer from the Si surface to the Au and H atoms. On the other hand, for a gas-phase Au–H molecule [Fig. 5(a)] and a Au–Si≡ moiety [Fig. 5(b)], the transfer of an electron to the electrophilic Au atom from the H or surface Si atom results in the spin pairing of Au, as seen in the corresponding Au LDOS plots (Fig. 5). The Au–H (in the Au–H molecule) and Au–Si (in the Au–Si≡ unit) bond lengths are $d_{Au-H} = 1.55$ Å and $d_{Au-Si} = 2.30$ Å, respectively, which are noticeably shorter than $d_{Au-H} = 1.64$ Å and $d_{Au-Si} = 2.38$ Å in the H–Au–Si≡ unit. This clearly demonstrates reduced Au–H and Au–Si interactions in the H–Au–Si≡ case. Indeed, the H–Au binding energy of 1.39 eV in the H–Au–Si≡, i.e., H–Au–Si≡ → ·H(gas)+Au–Si≡, is predicted to be far smaller than 2.98 eV as estimated for dissociation of a gas-phase Au–H molecule, i.e., H–Au → ·H+·Au.

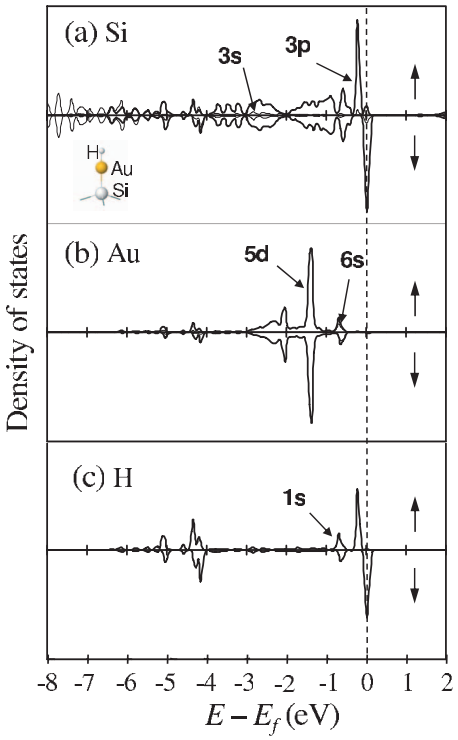

FIG. 4. Spin-polarized density of states projected onto the Si, Au, and H atoms in the H–Au–Si≡ unit, as indicated. For the Au and Si cases, the s and p states are indicated by thin and thick solid lines, respectively. The dashed vertical line at $E=0$ eV indicates the Fermi level.

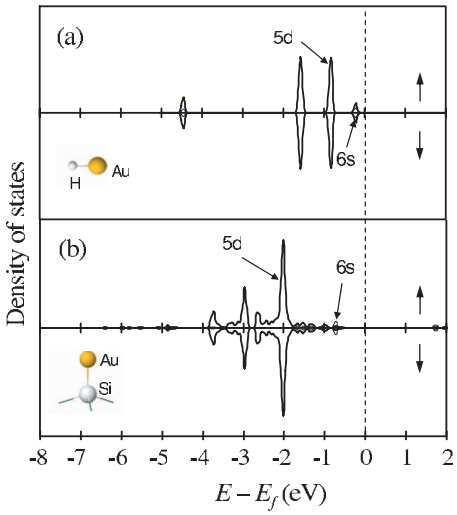

FIG. 5. Spin-polarized density of states projected onto the Au atom in (a) the H–Au molecule and (b) the Au–Si≡ unit, as illustrated by the corresponding insets. For the Au and Si cases, the s and p states are indicated by thin and thick solid lines, respectively. The dashed vertical line at $E=0$ eV indicates the Fermi level.

B. Diffusion

Next, we extensively examined Au diffusion on the H-terminated Si(111) surface considering various possible routes. Figure 6 shows a viable diffusion path starting from the most stable T site, together with an energy variation along the minimum-energy route. The Au atom moves out from the T site by interacting with a neighboring Si atom, followed by combination of the H and Si atoms to restore the original Si–H bond. The $T \rightarrow B$ transformation is predicted to require overcoming a barrier of 0.5 eV. Then, the move-out Au atom at the B site may either migrate to an adjacent B site through a threefold F or H site or move into the T site. According to our calculations, the F and H sites are identified to be saddle points, rather than stable adsorption sites. The predicted barriers for the $B \rightarrow F \rightarrow B$ and $B \rightarrow H \rightarrow B$ migrations are about 0.14 and 0.20 eV, respectively, which are lower than 0.24 eV for the $B \rightarrow T$ conversion. Taking the predicted barriers, the overall activation energy of Au diffusion is estimated to be 0.5 eV. The moderate cost implies that

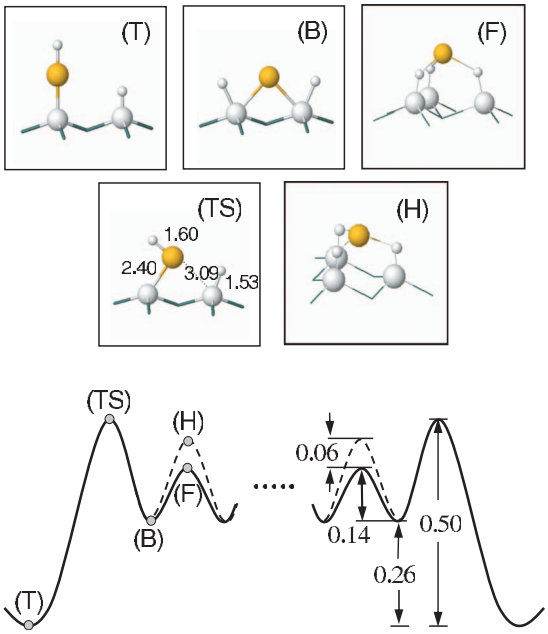

FIG. 6. Predicted diffusion pathways of Au on the H-terminated Si(111) surface. The energy variation is given in eV and the bond lengths indicated in the transition state (TS) are given in angstroms. The dark (yellow) gray, gray, and small white balls represent Au, Si, and H atoms, respectively. The diffusion routes were determined using NEBM with eight intermediate images for each diffusion step. Our search predicts that Au diffusion may follow move-out and move-in mechanisms; that is, a Au adatom that moves out from *T* to *B* may undergo migration across the H-terminated Si(111) surface through *H* or *F* until moving into *T*.

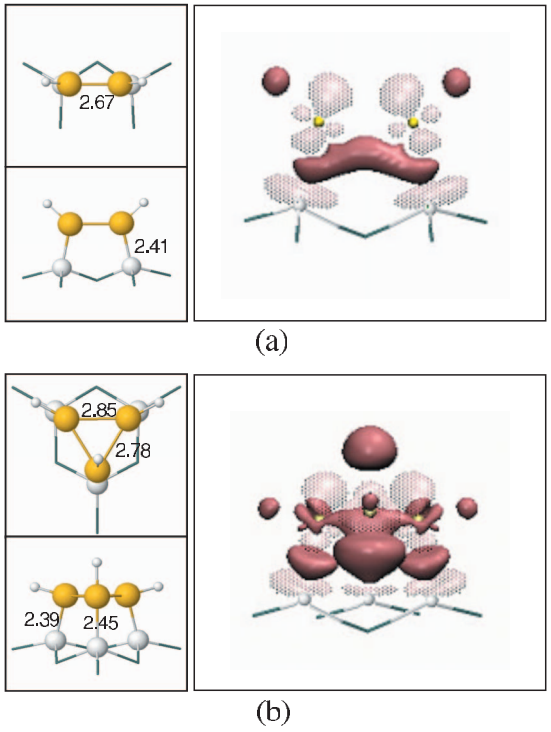

FIG. 7. Minimum energy configurations and corresponding charge density difference isosurfaces for (a) Au dimer and (b) Au trimer. The dark (yellow) gray, gray, and small white balls represent Au, Si, and H atoms, respectively. The bond lengths indicated are given in angstroms. Each charge density difference plot is obtained by subtracting the charge densities of the corresponding Au cluster (Au_n, $n=2$ or 3) and isolated H atoms from the total charge density of the $(H-Au)_n-Si\equiv$ unit with no atomic displacement, i.e., $\Delta\rho=\rho_{(H-Au)n\text{-}Si\equiv}-\rho_{Au_n}-\Sigma_n\rho_H$. The dark gray (brown) and gray isosurfaces represent the regions of charge gain and loss, respectively.

single Au atoms can migrate on Si(111)–H without disrupting Si–H bonds (under moderate temperature conditions where *H* decomposition barely occurs), consistent with earlier experimental observations.[11]

Our calculation results demonstrate that the Au diffusion may take place by moving in and out of the *T* site, which appears analogous to a kick-in and kick-out reaction for impurity diffusion in semiconductors. However, the kick-out diffusion model involves the conversion of a substitutional impurity to a mobile interstitial by capturing a self-interstitial atom. To distinguish from the well known kick-out mechanism, hereafter we refer to the Au diffusion mechanism as move-out and move-in mechanism.

C. Agglomeration

Finally, we looked at a very early stage of Au agglomeration on Si(111)–H. Earlier experiments[11–13] evidenced that deposited Au atoms agglomerate to form clusters far below room temperature (where Au-silicide formation is suppressed). Figure 7 shows minimum-energy configurations for Au dimer and trimer. The result demonstrates that H atoms favorably remain on the Au cluster surface rather than at the Au/Si interface, consistent with earlier experiments which ruled out the prevalence of H at the Au/Si(111) interface.[11] Similar to the Au monomer case (Fig. 3), for the small clusters analysis of bonding mechanisms based on charge density differences shows electron accumulation in the H atoms and electron depletion in the surface Si atoms, along with charge polarization of the deposited Au clusters. In addition, our calculations demonstrate the weak binding of H atoms to the clusters as well as the ease of associative H_2 desorption (see below).

In the dimer state [Fig. 7(a)], the Au–Au distance is 2.67 Å which close to 2.65 Å for a negatively charged Au dimer in the gas phase, rather than 2.54 Å in the neutral state. This indicates that the deposited Au dimer is negatively charged and there also exists a sizable interaction with the Si surface atoms. Like the monomer case, the H–Au and Au–Si lengths of 1.64 and 2.38 Å, respectively, are far greater than the corresponding lengths of 1.55 Å in gas-phase Au–H and 2.30 Å in $Au-Si\equiv$. The dimer state is predicted to be 0.81 eV more stable than when two monomers are fully separated. To look at the behavior of the weakly bound H atoms, we also performed *ab initio* molecular dynamics (AIMD) simulations at 300 K. The results show that the H atoms associatively desorb from the Au dimer within a picosecond, implying that the activation energy of the H_2 desorption is minimal. The associative H_2 desorption turns out to be exothermic by 1.05 eV, while the H–Au binding energy (on average) is estimated to be 1.68 eV. Upon the H_2 desorption, the Au–Au distance is elongated to 2.9 Å due to the increased Au–Si interaction [Fig. 8(a)].

As shown in Fig. 7(b), the trimer exhibits a distorted triangle structure, with $d_{Au-Au}=2.78-2.85$ Å and $d_{Au-Si}=2.39-2.45$ Å. The trimer yields an energy gain of 1.15 eV, over the dimer [Fig. 7(a)] plus the monomer [Fig. 2(a)]. Our

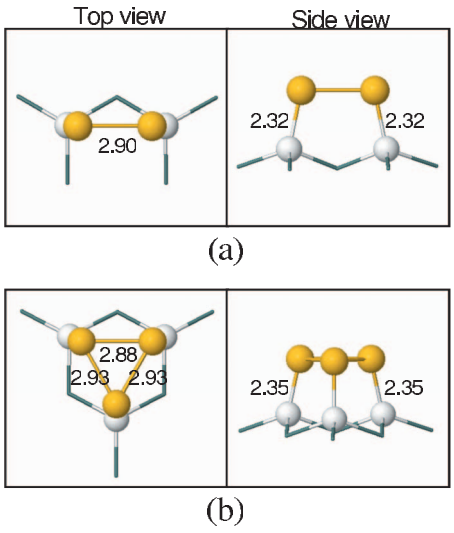

FIG. 8. Minimum energy configurations of (a) Au dimer and (b) Au trimer after H_2 and 3/2 H_2 desorption from the corresponding clusters (see Fig. 7). The dark (yellow) gray and gray balls represent Au and Si atoms, respectively.

AIMD shows that the weakly bound H atoms undergo significant thermal fluctuations. In the trimer state, the H–Au binding energy (on average) is estimated to be 1.85 eV, and the associative desorption of two H atoms (while leaving one H atom on the Au trimer) is predicted to be exothermic by 0.45 eV. After the H_2 desorption, the remaining H atom easily hops around on the Au trimer surface, while the H–Au binding strength reduces to 1.43 eV. Upon removal of the third H atom, the dehydrogenated Au trimer has an isotriangle configuration with $d_{\mathrm{Au-Au}}=2.88-2.93$ Å and $d_{\mathrm{Au-Si}}=2.35$ Å, while each Au atom terminates a Si dangling bond [Fig. 8(b)].

Here it is worth noting that the H–Au binding strength is a function of Au cluster size and H coverage. Moreover, the weak but sizable interaction of H atoms with the supported Au clusters may suggest the possibility of using small Au clusters deposited on the H-terminated Si(111) surface for catalytic hydrogenation and hydrogen storage. A further investigation of the interaction of hydrogen species with larger Au clusters $(\mathrm{Au}_n, n \geq 4)$ supported on Si(111)–H is underway.

IV. SUMMARY

We present the adsorption, diffusion, and agglomeration of Au atoms on the H-terminated Si(111)-(1×1) surface based on periodic slab DFT calculations. Our calculations show that a single Au atom preferentially resides at the one-fold top (T) site in which the Au atom is directly bonded to a surface Si atom while breaking an original Si–H bond, and the H atom is attached to the top of the adsorbed Au atom rather than the surface Si atom. The resulting energy gain is predicted to be 0.91 eV with respect to a gas-phase Au atom in the doublet ground state. For the T-site Au adsorption, analysis of bonding mechanisms based on charge density differences shows existence of ionic-type Si–Au and Au–H interactions. Starting from the most stable T site, Au diffusion is predicted to occur via a series of move-out and move-in events. That is, the Au atom moves out from the T site by interacting with a neighboring Si atom, leading to restoration of the original Si–H bond. The move-out Au atom undergoes migration across the H-terminated Si(111) surface until moving into the T site. The overall activation energy of the Au diffusion that follows move-out and move-in mechanisms is predicted to be 0.5 eV, which is substantially higher than that ($\approx$0.15 eV) for Ag migration that likely proceeds over the topmost H atoms. The calculation results explicitly demonstrate that single Au atoms will migrate on Si(111)–H without disrupting Si–H bonds at temperatures far below 450 °C at which H decomposition may happen. We also report the atomic configurations, thermal stability, and bonding mechanisms of small Au clusters (such as dimer and trimer). The results demonstrate that H atoms favorably remain on the Au cluster surface rather than at the Au/Si interface; the H atoms are weakly bound to the Au clusters and easily undergo associative H_2 desorption with no significant barrier. Our findings are as a whole consistent with earlier experimental observations[11] such as liberation of H atoms from the Au/Si(111) interface, no diffusion-induced disruption of H–Si bonds, and low mobility of Au adatoms, compared to other metals such as Ag that undergo migration over the H adlayer, rather than following the move-out and move-in mechanism. The improved fundamental understanding will contribute to precise design and fabrication of various nanoscale devices and systems based on Au–Si alloys.

ACKNOWLEDGMENTS

We acknowledge Robert A. Welch Foundation (F-1535) for their financial support. All our calculations were performed using supercomputers in the Texas Advanced Computing Center at the University of Texas at Austin.

[1] W. F. Egelhoff, Jr. and D. A. Steigerwald, J. Vac. Sci. Technol. A **7**, 2167 (1989).
[2] K. Sumitomo, T. Kobayashi, F. Shoji, and K. Oura, Phys. Rev. Lett. **66**, 1193 (1991).
[3] M. Naitoh, F. Shoji, and K. Oura, Jpn. J. Appl. Phys., Part 1 **31**, 4018 (1992).
[4] K. Murano and K. Ueda, Surf. Sci. **357–358**, 910 (1996).
[5] A. Nishiyama, G. ter Horst, P. M. Zagwijn, G. N. van den Hoven, J. W. M. Frenken, F. Garten, A. R. Schlatmann, and J. Vrijmoeth, Surf. Sci. **350**, 229 (1996).
[6] T. Yasue and T. Koshikawa, Surf. Sci. **377–379**, 923 (1997).
[7] F. Houzay, G. M. Guichar, A. Cros, F. Salvan, R. Pinchaux, and J. Derrien, J. Phys. C **15**, 7065 (1982).
[8] C. L. Kuo and P. Clancy, Surf. Sci. **551**, 39 (2004).
[9] S. H. Lee and G. S. Hwang, J. Chem. Phys. **127**, 224710 (2007).
[10] Y. Wu, Y. Cui, L. Huynh, C. J. Barrelet, D. C. Bell, and C. M. Lieber, Nano Lett. **4**, 433 (2004).
[11] M. Wilde and K. Fukutani, Jpn. J. Appl. Phys., Part 1 **42**, 4650 (2003).
[12] C. Grupp and A. Taleb-Ibrahimi, Phys. Rev. B **57**, 6258 (1998).
[13] L. A. Gheber, M. Hershifinkel, G. Gorodetsky, and V. V. Olterra, Thin Solid Films **320**, 228 (1998).
[14] K. Fukutani, H. Iwai, Y. Murata, and H. Yamashita, Phys. Rev. B **59**, 13020 (1999).
[15] H. J. Jeong and S. M. Jeong, Phys. Rev. B **73**, 125343 (2006).
[16] J. B. Hannon, S. Kodambaka, F. M. Ross, and R. M. Tromp, Nature (London) **440**, 69 (2006).
[17] U. Gosele, Nature (London) **440**, 34 (2006).
[18] S. Kodambaka, J. Tersoff, M. C. Reuter, and F. M. Ross, Phys. Rev. Lett. **96**, 096105 (2006).
[19] T. Kawashima, T. Mizutani, T. Nakagawa, H. Torri, T. S. Aitoh, K.

Komori, and M. Fujii, Nano Lett. **8**, 362 (2008).
[20] N. A. Stolwijk, B. Schuster, and J. Holzl, Appl. Phys. A: Mater. Sci. Process. **33**, 133 (1984).
[21] J. Perdew, J. Chevary, S. Vosko, K. Jackson, M. Pederson, D. Singh, and C. Fiolhais, Phys. Rev. B **46**, 6671 (1992).
[22] G. Kresse and J. Hafner, Phys. Rev. B **47**, 558 (1993).
[23] G. Kresse and J. Furthmüller, Comput. Mater. Sci. **6**, 15 (1996).
[24] G. Kresse and J. Furthmüller, Phys. Rev. B **54**, 11169 (1996).
[25] D. Vanderbilt, Phys. Rev. B **41**, 7892 (1990).
[26] G. Kresse and J. Hafner, J. Phys.: Condens. Matter **6**, 8245 (1994).
[27] G. Henkelman, B. P. Uberuaga, and H. Jonsson, J. Chem. Phys. **113**, 9901 (2000).